Edinburgh Research Explorer

Huntingtin proteolysis releases non-polyQ fragments that cause toxicity through dynamin 1 dysregulation

Article

Huntingtin proteolysis releases non-polyQ fragments that cause toxicity through dynamin 1 dysregulation

Marie-Thérèse El-Daher[1,2,3,†], Emilie Hangen[1,2,3,†], Julie Bruyère[1,2,3,4,5], Ghislaine Poizat[1,2,3], Ismael Al-Ramahi[6,7], Raul Pardo[1,2,3], Nicolas Bourg[8,9], Sylvie Souquere[10,11], Céline Mayet[8,9], Gérard Pierron[10,11], Sandrine Lévêque-Fort[8,9], Juan Botas[6,7], Sandrine Humbert[1,2,3,4,5,*] & Frédéric Saudou[1,2,3,4,5,12,**]

Abstract

Cleavage of mutant huntingtin (HTT) is an essential process in Huntington's disease (HD), an inherited neurodegenerative disorder. Cleavage generates N-ter fragments that contain the polyQ stretch and whose nuclear toxicity is well established. However, the functional defects induced by cleavage of full-length HTT remain elusive. Moreover, the contribution of non-polyQ C-terminal fragments is unknown. Using time- and site-specific control of full-length HTT proteolysis, we show that specific cleavages are required to disrupt intramolecular interactions within HTT and to cause toxicity in cells and flies. Surprisingly, in addition to the canonical pathogenic N-ter fragments, the C-ter fragments generated, that do not contain the polyQ stretch, induced toxicity via dilation of the endoplasmic reticulum (ER) and increased ER stress. C-ter HTT bound to dynamin 1 and subsequently impaired its activity at ER membranes. Our findings support a role for HTT on dynamin 1 function and ER homoeostasis. Proteolysis-induced alteration of this function may be relevant to disease.

See also: **M Jimenez-Sanchez & DC Rubinsztein** (September 2015)

Introduction

Huntington's disease (HD) is a devastating autosomal dominant inherited neurodegenerative disorder characterised by personality changes, cognitive deterioration, involuntary choreiform movements and hypokinesia. HD neuropathology involves the preferential loss of neurons from the striatum and the cortex. There is currently no effective treatment to delay or prevent disease progression. HD is caused by an abnormal polyglutamine (polyQ) expansion at the extreme N-terminus (N-ter, amino acid 18) of the protein huntingtin (HTT), a large protein of 3,144 amino acids (aas). Although the mechanisms that lead to HD are not fully understood, a series of events that ultimately lead to the death of neurons in the brain have been described (Cattaneo *et al*, 2005; Borrell-Pages *et al*, 2006; Imarisio *et al*, 2008).

A crucial step in HD pathogenesis is the cleavage of full-length HTT releasing smaller N-ter fragments that contain the polyQ stretch and that are toxic to neurons. Such polyQ-containing fragments have been consistently observed in human HD brains and HD mouse models (Kim *et al*, 2001; Mende-Mueller *et al*, 2001; Wellington *et al*, 2002; Wang *et al*, 2008; Landles *et al*, 2010). Several proteases, including caspases, calpains, cathepsins and metalloproteinases, that cleave HTT have been reported (Goldberg *et al*, 1996; Kim *et al*, 2001, 2006; Gafni & Ellerby, 2002; Lunkes *et al*, 2002; Hermel *et al*, 2004; Ratovitski *et al*, 2009; Miller *et al*, 2010; Tebbenkamp *et al*, 2012), and inhibition of HTT cleavage reduces toxicity both *in vitro* and *in vivo* (Wellington *et al*, 2000; Gafni *et al*, 2004; Graham *et al*, 2006; Miller *et al*, 2010). PolyQ

1 Institut Curie, Orsay, France
2 CNRS, UMR3306, Orsay, France
3 INSERM, U1005, Orsay, France
4 Inserm, U836, Grenoble, France
5 Grenoble Institut des Neurosciences, GIN, University of Grenoble Alpes, Grenoble, France
6 Department of Molecular and Human Genetics, Baylor College of Medicine, Houston, TX, USA
7 Jan and Dan Duncan Neurological Research Institute, Texas Children's Hospital, Houston, TX, USA
8 ISMO, CNRS, UMR8214, University of Paris Sud, Orsay, France
9 CPBM, FR2764, University of Paris Sud, Orsay, France
10 CNRS, UMR8122, Villejuif, France
11 Institut Gustave Roussy, Villejuif, France
12 CHU de Grenoble, Grenoble, France
*Corresponding author. Tel: +33 456 52 06 29; E-mail: sandrine.humbert@inserm.fr
**Corresponding author. Tel: +33 456 52 05 14; E-mail: frederic.saudou@inserm.fr
†These authors contributed equally to this work

N-ter fragments can reproduce several aspects of the disease. For example, a fragment corresponding to Exon1, containing the polyQ stretch, is sufficient to induce a neurological phenotype in mouse (Mangiarini *et al*, 1996). Consequently, such N-ter fragments have been extensively used to study HD. Toxicity expressed by N-ter fragments requires their nuclear translocation (Saudou *et al*, 1998); this causes transcriptional dysregulation detrimental to neuronal survival (Sugars & Rubinsztein, 2003; Landles & Bates, 2004). Mutant HD fragments also induce neuronal dysfunctions, including defects in signal transduction, autophagy and both calcium and mitochondrial homoeostasis (for reviews, see Borrell-Pages *et al*, 2006; Imarisio *et al*, 2008; Li & Li, 2010). Together, these studies have established that N-ter fragment(s) containing the polyQ stretch are the crucial factors responsible for HD pathogenesis.

However, the cascade of proteolytic events leading to the generation of these toxic fragments is unclear. Also, the precise consequences of full-length HTT proteolysis at the molecular and cellular levels are unknown. This could be partly due to the complexity to monitor HTT proteolysis. Also, the reasons why some N-ter fragments are more toxic than others are obscure. One consensus theory is that these mutant fragments are more toxic the shorter they are (Hackam *et al*, 1998; Landles *et al*, 2010), but this does not explain why some proteolytic cleavages are more toxic than others, independently of any major difference in the sizes of the resulting fragments (Graham *et al*, 2006). Also, HTT is cleaved by numerous proteases, some of which have not yet been identified (Lunkes *et al*, 2002; Gafni *et al*, 2012). Finally, activating a specific protease will induce the cleavage of many substrates besides HTT itself. This makes it difficult to determine the consequences of individual cleavages. Although N-ter fragments recapitulate features of HD in cells and *in vivo*, such models only incompletely reproduce what is observed in patients with HD. Indeed, in human HD, the full-length protein is present from early stages; consequently, any HTT cleavage generating short N-ter fragments (amino acid positions ranging from 1–105 to 1–586) will also generate corresponding C-ter fragments. Such C-ter fragments are observed in post-mortem HD brain samples (Mende-Mueller *et al*, 2001; Landles *et al*, 2010), but their contribution, if any, to the pathogenic process has not been studied.

Here, we report the development of a time- and site-specific controlled system for HTT proteolysis *in vitro* and *in vivo*. We used this system to investigate the consequences of proteolysis of full-length mutant HTT and the generation of both N-ter and C-ter fragments on neuronal survival *in vitro* and *in vivo*. We report that cleavage of HTT releases a C-terminal HTT that impairs dynamin 1 activity leading to endoplasmic reticulum stress and cell death.

Results

Time- and site-specific control of huntingtin proteolysis

Studies focusing on HTT cleavage and toxicity have used either protease inhibitors mutated the sites to become non-cleavable ones or expressed truncated fragments containing the polyQ stretch. To recapitulate the cleavage of full-length HTT occurring in cells, we took advantage of the ability of the tobacco etch virus (TEV) protease to specifically cleave engineered proteins that contain a

seven amino acid sequence that is not present in the mammalian proteome but is recognised by the TEV protease. As a proof of concept for HTT-specific proteolysis, we generated full-length HTT constructs in which the putative caspase-6 site (position 586), caspase-3 site (513) and Cp2 site (167) are replaced by a TEV recognition cleavage site (TEVrcs) (Fig 1A) as cleavage at these sites has been implicated in HD pathogenesis (Wellington *et al*, 2000; Graham *et al*, 2006; Ratovitski *et al*, 2011). We validated our system by expressing the various HTT-TEV constructs in HEK293T cells and incubating protein extracts with an excess of recombinant TEV protease. Whereas TEV protease was unable to cleave polyQ FL-HTT constructs that did not contain the TEVrcs (referred to as "no TEV"), it efficiently cleaved all of polyQ FL-HTT586TEV, FL-HTT513TEV, FL-HTT167TEV (Fig EV1A). HTT proteolysis in patient brains is the result of a combination of various cleavage events, so we also generated constructs containing two TEVrcs (Fig 1A). Incubation of these constructs with recombinant TEV generated proteolytic fragments of the expected sizes including intermediate fragments that are those which are cleaved at only one site (Fig EV1A). We next assessed whether inserting the TEV sequences in HTT influenced protein toxicity and function. First, we found that the presence of the TEV sequence (without proteolysis induction) at positions 586, or 167 and 586 had no major effect on the toxicity of the polyQ FL-HTT constructs (Fig EV1B). We next focused on HTT function in Golgi maintenance as this function is (i) well described (Caviston *et al*, 2007; Pardo *et al*, 2010) and (ii) depends on HTT interaction with dynein/dynactin complex in the N-terminal region of HTT (regions 171–230 and 536–698 that are close to or contain the TEV sites). We therefore silenced endogenous HTT in HeLa cells and tested whether re-expressing siRNA-insensitive HTT constructs containing two TEV sites were able to reassemble Golgi ribbons. The wild-type HTT containing two TEV sites reformed intact Golgi apparatus after nocodazole wash out to the same extent as the FL-HTTQ23 without TEV sites. And similarly to the polyQ-HTT inability to reassemble the Golgi apparatus (Pardo *et al*, 2010), the polyQ-HTT containing two TEV sites was unable to do so. We conclude that HTT with two TEV sites remains functional on its dynein/dynactin scaffolding function (Fig EV1C).

We next analysed the proteolysis of these HTT constructs in cells using the inducible SNIPer-TEV system. This system involves two vectors encoding the N and C parts of the TEV fused to FRB and FKBP fragments, respectively. Addition of 10 or 20 nM of rapamycin induces a rapid heterodimerisation of the fragments and thereby expression of the TEV protease activity (Gray *et al*, 2010). We treated HEK293T cells expressing the HTT-TEV and the SNIPer-TEV constructs with 20 nM rapamycin and analysed proteolysis at 24 h. Rapamycin at this concentration had no effect on proteolysis of endogenous HTT or on its toxicity. Whereas 80–95% of FL-HTT constructs were cleaved at positions 513 or 586 (Fig 1B), proteolysis at position 167 did not occur efficiently unless if HTT was also cleaved at positions 513 or 586, suggesting that the proteolytic cleavage sites in HTT are not all equally accessible.

We next compared the proteolysis of WT versus polyQ-HTT at position 167 in the striatal ST*Hdh* cell line referred after as striatal cells (Trettel *et al*, 2000). We confirmed that for both WT and polyQ constructs, cleavage at position 586 enhanced cleavage at position 167 (Fig 1C). Also, the presence of a polyQ stretch in HTT slightly
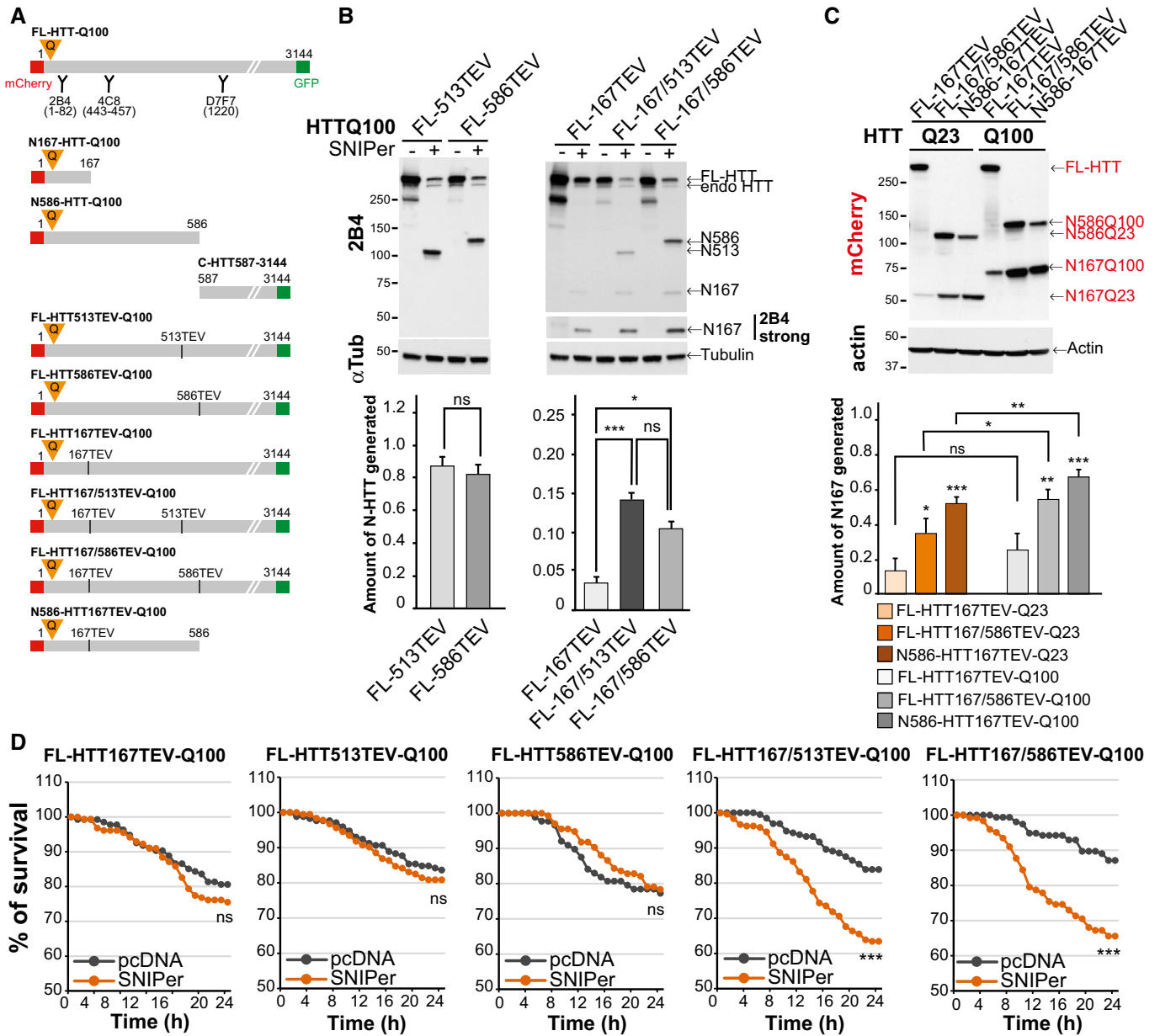
Figure 1. Sequential proteolysis of huntingtin reveals toxic events.

A   Schematic representations of N-ter, C-ter or full-length polyQ-HTT constructs used and location of antibody epitopes and tags.
B   Analyses of HTT N-ter fragments generated after cleavage of the indicated HTT-TEV-Q100 constructs by the SNIPer-TEV in HEK293T cells at 24 h.
C   Analyses of HTT N167 fragments generated upon cleavage of wild-type and mutant HTT (24 h) in striatal cells.
D   Survival of striatal cells upon SNIPer-TEV-induced cleavage of FL-HTT-TEV-Q100.

Data information: The bar graphs (mean ± SEM) display pooled data from four (B) or five (C) independent experiments. For (D), the total numbers of cells and number of independent experiments are as follows: FL-HTT167TEV+pcDNA: 134 or +SNIPer: 155 ($n = 3$), FL-HTT513TEV+pcDNA: 171 or +SNIPer: 183 ($n = 4$), FL-HTT586TEV+pcDNA: 88 or +SNIPer: 134 ($n = 3$), FL-HTT167/513TEV+pcDNA: 155 or +SNIPer: 122 ($n = 3$), FL-HTT167/586TEV+pcDNA: 192 or +SNIPer: 238 ($n = 4$). Statistics were done by unpaired t-test with Welch's correction $P = 0.5730$ (B, left panel), one-way ANOVA with Bonferroni's multiple comparison (B, right panel), one-way ANOVA with Fisher LSD test and one-way ANOVA with paired t-test (C), Kaplan–Meier, log-rank test (D). ns: non-significant, *$P < 0.05$, **$P < 0.01$, ***$P < 0.001$. See also Fig EV1.

favoured the production by proteolysis of the N167 fragment, suggesting that polyQ expansion may render the 167 site more accessible. Our findings validate the use of the TEV approach to study intrinsic proteolytic properties of HTT. It also suggests that HTT is subject to a proteolytic cascade that may be more efficient when HTT contains a pathogenic expanded polyQ stretch.

Sequential proteolysis accelerates huntingtin toxicity

We used the striatal cells to analyse the toxicity associated with HTT proteolysis at particular positions. We transfected the cells with the various HTT-TEV constructs and the two SNIPer-TEV plasmids or an empty pcDNA vector as a control; 20 h later, 10 nM of

rapamycin was added to transfected cells, identified by the presence of the mCherry tag on HTT constructs. The fate of individual cells containing HTT was then followed for 24 h by robotic automated videomicroscopy. Expression of the SNIPer-TEV or rapamycin treatment had no significant effect on non-cleavable HTT constructs (Fig EV1D). We next analysed the toxicity of the various constructs upon cleavage (Fig 1D). The FL-HTT167TEV-Q100 construct displayed no obvious toxicity (Figs 1D and EV1D); this is consistent with the poor efficiency of cleavage at position 167 by TEV. Surprisingly, cleavage of the constructs with TEVrcs at positions 513 and 586 had no evident effect on cell survival (Figs 1D and EV1D) although proteolysis of these HTT constructs was very efficient (Fig 1B and C). In contrast, double cleavage at sites 586/167 or 513/167 led to a significant increase in polyQ-HTT-induced toxicity compared to each site alone (Figs 1D and EV1D and Movie EV1). These results suggest that cleavage at 513 or 586 sites has no immediate consequences on polyQ-mediated toxicity. Rather, the sequential proteolysis promotes mutant HTT-induced toxicity.

Huntingtin intramolecular interaction is lost upon specific proteolysis

N-terminal regions of HTT interact with more C-terminal regions (Palidwor *et al*, 2009). Since cleavage at 513 and 586 gave similar results, we focused on 586 site and tested whether N586 fragment and the C-HTT587-3144 fragment interacted. Using brain extracts from heterozygous $Hdh^{Q7/Q111}$ mice treated *in vitro* with recombinant caspase-6, we found that the C-HTT587-3144 fragment interacted with the N586 fragment and that this interaction was not affected by the polyQ expansion (Fig 2A). We next expressed simple or double FL-HTT-TEV constructs with the SNIPer-TEV system in HEK293T cells and treated cells for 24 h with 20 nM rapamycin to induce HTT proteolysis. C-ter fragments produced by cleavage at position 586 co-immunoprecipitated the corresponding wild-type and polyQ N586 fragments. However, there was no interaction between the C-HTT587-3144 fragments and the N167 fragments (Figs 2B and EV2A). We conclude that polyQ N586 fragments interact with their corresponding C-ter fragments, but that further proteolysis of the N-ter fragment abolishes the interaction.

To further investigate the physiological relevance of increased proteolysis and loss of HTT intramolecular interaction, we analysed the presence of N-ter and C-ter fragments in post-mortem striatal brain samples from patients with HD and control individuals (Fig 2C). In control samples, we detected full-length HTT as well as

C-ter and N-ter fragments of approximate sizes of 250 and 70 kDa, respectively. These fragments may correspond to HTT proteolysis in the 500- to 600-amino acid region of HTT, and they have been previously reported in control samples (Kim *et al*, 2001; Mende-Mueller *et al*, 2001; Gafni & Ellerby, 2002; Lunkes *et al*, 2002; Wellington *et al*, 2002; Hermel *et al*, 2004; Landles *et al*, 2010). Interestingly, the 250 and 70 kDa fragments may correspond to the C-HTT587-3144 and N586-HTT fragments generated after single TEV proteolysis (Figs 2A and B and EV2A). In HD post-mortem striatal brain samples, we found a lower level of full-length HTT compared to control individuals. We also detected the C-ter fragment of 250 kDa as well as large amounts of N-ter fragments that are smaller than the 70 kDa fragment observed in control samples. This increased level of very small N-ter fragments recognised only by the 2B4 antibody and the loss of the 70 kDa N-ter fragment suggest an increased proteolysis of the 70 kDa fragment. However, we cannot exclude that part of these fragments might be generated by repeat length-dependent alternative splicing (Sathasivam *et al*, 2013). Because we observed in cells that the C-HTT587-3144 fragment interacted with the N586 but not shorter ones, we investigated whether increased proteolysis in HD samples leads to loss of intramolecular interaction and perform immunoprecipitation experiments of brain samples using anti C-ter HTT antibody (D7F7) (Fig 2C, right panel). Whereas the C-ter antibody co-immunoprecipitated the large 70 kDa N-ter fragment in striatal brain samples from control individuals, no shorter fragments were detected in the striatal brain samples from HD individuals. We conclude that in HD situation, the C-ter fragment, although less abundant than in control situation, is potentially free from its intramolecular interaction with N-ter fragments (Fig 2D).

Both N- and C-terminal huntingtin fragments induce toxicity that depends on the size of N-terminal fragments

To further study the relation between intramolecular interaction and toxicity, we generated constructs that mimic the different fragments generated after HTT cleavage at 586 and expressed them in HeLa or striatal cells (Fig EV2B and C). As shown by immunoprecipitation, the N586 fragment but not the short N167 one interacts with the C-HTT587-3144 fragment (Fig EV2B). As expected (Hackam *et al*, 1998), N167-HTTQ100 is more toxic than N586-HTTQ100 (Fig 2E). Interestingly, co-expression of C-HTT587-3144 construct potentiated the toxicity induced by the N167-HTTQ100 fragment but had no effect on that of the N586-HTTQ100 fragment (Figs 2E and EV2C).

Figure 2. Intramolecular interactions between proteolytic huntingtin fragments.

A Protein lysates from $Hdh^{Q7/Q111}$ mouse brains were cleaved with recombinant caspase-6, and generated N-ter and C-ter fragments were subjected to immunoprecipitation.

B Immunoprecipitation performed in HeLa cells upon cleavage of FL-HTT-TEV-Q100. # indicates a non-specific band.

C Immunoblotting analysis of HTT proteolysis and co-immunoprecipitation of HTT C-ter and N-ter fragments in post-mortem control and HD human striatum samples. Asterisks indicate the position of small N-ter fragments.

D Schematic representation of antibody epitope locations and interactions between various HTT fragments generated in cells and in human brain samples.

E Cell death induced by the indicated HTT constructs in transfected striatal cells.

F Survival curves of striatal cells upon cleavage of FL-HTT-TEV-Q23.

Data information: The bar graphs (mean ± SEM) display pooled data from 3 independent experiments in triplicates (E). For (F), the total numbers of cells and number of independent experiments are as follows: FL-HTT-Q23 + pcDNA: 97 + SNIPer: 120 (*n* = 2), FL-HTT167/586TEV-Q23 + pcDNA: 200 + SNIPer: 199 (*n* = 4). Statistics were done by one-way ANOVA with Bonferroni's multiple comparison tests (E) and Kaplan–Meier, log-rank test (F). ns: non-significant, **P < 0.01, ***P < 0.001. See also Fig EV2.
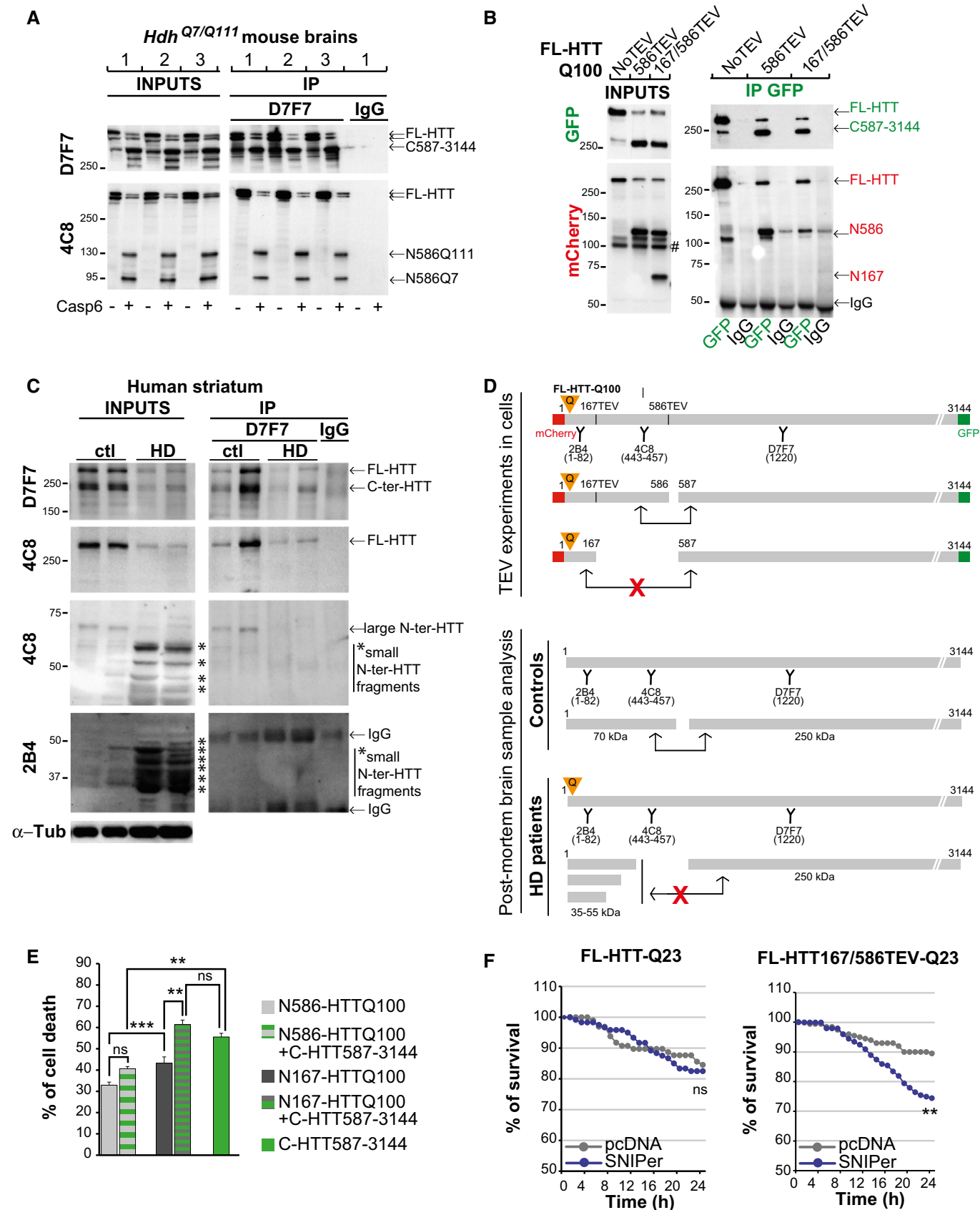
Figure 2.

We also measured the toxicity of the C-HTT587-3144 fragment alone in striatal cells. Surprisingly, it was highly toxic and even more toxic than the N167-HTTQ100 fragment (Fig 2E). As such fragments are also generated upon wild-type FL-HTT cleavage, inducing artificially the cleavage of wild-type FL-HTT should also lead to toxicity. Indeed, whereas TEV activation had no effect on FL-HTT-Q23, it significantly increased toxicity of WT-FL-HTT with TEV sites at positions 167 and 586 (Fig 2F). Since the C-ter fragment when expressed alone induced some toxicity, we tested the possibility that this could occur through a dominant-negative effect on full-length endogenous HTT that is present in cells. We therefore expressed FL-HTT167/586TEV-Q23 and FL-HTT167/586TEV-Q100 constructs in cells silenced or not for endogenous HTT and induced cleavage by SNIPer-TEV activation (Fig EV2D). We found no difference in the toxicity upon HTT double proteolysis whether endogenous HTT was present or downregulated. We conclude that in addition to mutant N-ter fragments, C-ter fragments generated from either wild-type or mutant HTT cleavage are toxic. The interaction of N-ter and C-ter fragments prevents them from being toxic.

C-terminal huntingtin fragment causes endoplasmic reticulum-derived vacuolation, stress and toxicity

To study the consequences of the loss of N–C interactions as N-ter fragments become shorter (as this is the case in post-mortem HD samples), we determined the localisation of C-HTT587-3144 with N586-HTTQ100 or N167-HTTQ100 in striatal cells. In agreement with biochemical findings (Fig 2), C-HTT587-3144 (GFP) co-localised with N586-HTTQ100 (mCherry) but less with N167-HTTQ100 (Fig 3A). As the interaction between the C-HTT587-3144 fragment and the short N-terminal fragments weakened, the proportion of the N-ter fragments in the nucleus increased; the C-ter fragment remained in the cytoplasm in all cases (Fig 3A). These findings are in agreement with previous reports showing an inverse correlation between nuclear localisation and the size of the N-ter fragments (Hackam *et al*, 1998; Saudou *et al*, 1998). When analysing cells at longer time points (24 h), large cytoplasmic vacuoles developed in cells producing both the C-HTT587-3144 fragment and the short non-interacting fragments (N167-HTTQ100) or producing the C-ter fragment alone (Fig 3B). These vacuoles were less frequent in cells producing the C-HTT587-3144 fragment and the N586-HTTQ100 fragment. No such vacuolar phenotype was observed in cells producing one of the polyQ N-ter HTT fragments alone (Fig 3B). Vacuoles formed around 36 h post-transfection and death occurred rapidly after the vacuoles started to emerge (11 h ± 0.8; *n* = 26 cells) (Movie EV2), suggesting a fast and dynamic process consistent with the kinetics of death observed following HTT-induced proteolysis (Fig 1).

We investigated the nature of the C-HTT587-3144 fragment-induced vacuoles. They were immuno-negative for GM130, CTR 433, TGN38, Rab5 and EEA1 (Fig EV3A) and are therefore unlikely to be derived from the Golgi apparatus, the trans-Golgi network or early endosomes. In addition, the vacuoles did not localise with LC3-GFP and LAMP2, suggesting they are not linked to autophagosomes or lysosomes (Fig EV3A). However, the C-terminal HTT-induced vacuoles were stained by antibodies for calnexin and ATF6, both chaperone proteins found in the endoplasmic reticulum (ER) membranes (Fig 3C). To confirm the role of the C-ter fragment in

the formation of these ER-derived vacuoles, we SNIPer-TEV-induced proteolysis of the FL-HTT167/586TEV-Q100 and Q23 constructs. As in cells expressing the C-HTT587-3144 construct, double proteolysis of both WT and mutant HTT was associated with dilation of the ER (in more than half the cells) and the emergence of cytoplasmic vacuoles (Fig 3D). We also co-expressed the C-HTT587-3144 fragment with a vector encoding GFP fused to the KDEL motif, a luminal marker of the ER: the vacuoles progressively filled with GFP-KDEL (Fig 3E and Movie EV3). Finally, C-HTT587-3144 fragment increased calnexin and BIP protein levels; it also led to an upregulation of full-length and truncated nuclear ATF6 (Fig 3F). Our data thus support that the C-HTT587-3144 fragment of HTT causes ER dilation and the formation of cytoplasmic vacuoles.

What is the death pathway elicited by C-ter HTT? Caspase inhibitors did not block cell death and C-ter-expressing cells were TUNEL negative (Fig EV3B–D). Also, Beclin-1 silencing failed to reduce cellular toxicity (Fig EV3E). Together, these data suggest that apoptosis and autophagy are unlikely to be directly involved. In contrast, treatment with the ER stress inhibitor salubrinal significantly decreased cell death among C-HTT587-3144-containing cells; it also resulted in an increase in the percentage of cells containing vacuoles (Fig 3G). Therefore, ER-derived vacuoles in C-HTT587-3144-containing cells induce ER stress and toxicity.

ER stress and vacuolation are observed in Huntington's disease knock-in mice

FL-HTT is proteolysed to give C-ter and N-ter fragments in brains of patients with HD and HD knock-in mouse models (Mende-Mueller *et al*, 2001) (Fig 2A and C). Therefore, the consequences of the putative C-ter fragment-associated toxicity we describe, such as ER stress activation and dilated ER, should also present in the brains of HD knock-in mice, in which mutant huntingtin is expressed at endogenous levels. We analysed ER stress signalling in the striata from 20-month-old $Hdh^{Q111/Q111}$ mice: nuclear ATF6 abundance and eif2α phosphorylation were significantly higher in mutant $Hdh^{Q111/Q111}$ than control wild-type $Hdh^{Q7/Q7}$ mice (Fig 4A). Next, we used electron microscopy to study the striatum of 20-month-old $Hdh^{Q111/Q111}$ mice. We found a significantly higher number of neurons showing swollen ER tubules in the striatum of $Hdh^{Q111/Q111}$ mice as compared to $Hdh^{Q7/Q7}$ mice (Fig 4B). Such dilation is reminiscent of ER dilation and vacuolation observed in striatal cells expressing the C-HTT587-3144 fragment (Figs 3 and 4B). These various findings suggest a possible toxic effect of C-ter fragments inducing ER stress and vacuolation *in vivo*.

HTT proteolysis and the presence of C-ter huntingtin lead to neurodegeneration in flies

We used *Drosophila* as a model to assess the relevance of our findings *in vivo* as expression of TEV has been successfully used in flies for proteolysis of proteins *in vivo* and showed no long-term effects (Harder *et al*, 2008; Pauli *et al*, 2008). Also, full-length transgenic models of HD have been previously reported (Romero *et al*, 2008), and HTT functions are conserved between flies and mammals (Godin *et al*, 2010; Zala *et al*, 2013). We generated a set of fly strains by site-directed insertion of FL-HTT constructs with 200Q; thus, all transgenic strains showed similar expression of the
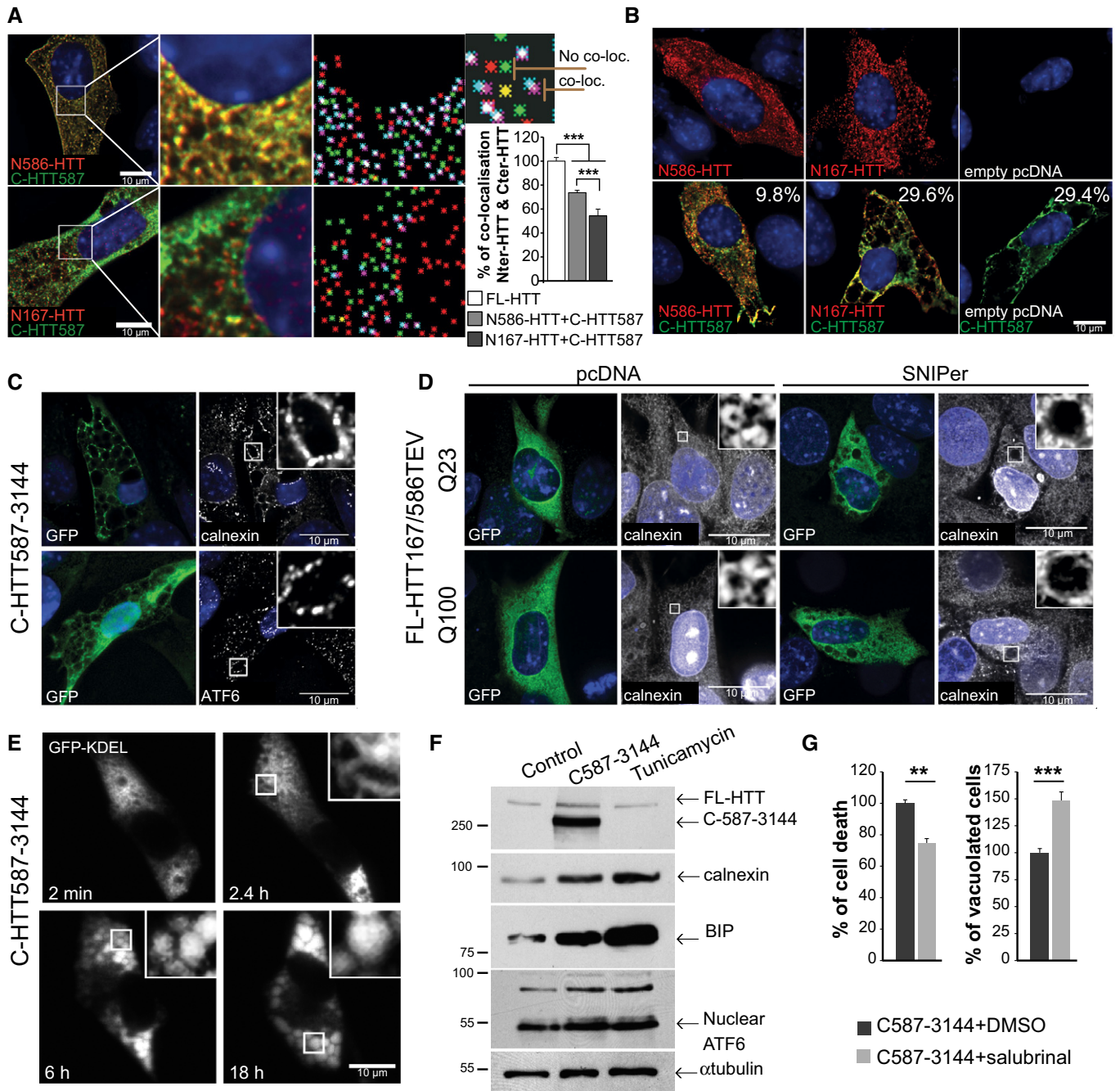
Figure 3.   Released C-terminal huntingtin fragment elicits endoplasmic reticulum dilation, stress and cell death.

A   Immunostaining of striatal cells transfected with C-HTT587-3144 (GFP) and N-HTTQ100 constructs (mCherry). Co-localisation was measured using the JACoP plugin (ImageJ, see Appendix Supplementary Materials and Methods). Maps illustrating the mass centre of particles from the two fluorophores are shown in the right column. Loc stands for localisation. Graph indicates the mean percentage of co-localisation between fragments. mCherry- and GFP-tagged FL-HTT are used as reference (100%).

B   Immunostaining of striatal cells expressing the indicated constructs. Values indicate the percentage of cells undergoing cytoplasmic vacuolation.

C   C-HTT587-3144-expressing striatal cells immunostained with anti-calnexin and anti-ATF6 antibodies.

D   Immunostaining of calnexin shows ER dilation upon cleavage of HTT167/586TEV-Q100 or Q23 (anti-GFP) in striatal cells.

E   Time-lapse imaging of luminal ER marker (GFP-KDEL) in a C-HTT587-3114-expressing striatal cells.

F   ER stress chaperones are upregulated in C-HTT587-3144-GFP striatal cells. Tunicamycin was used as a control for ER stress.

G   Cell death and vacuolation after treatment with salubrinal, an ER stress inhibitor in striatal cells.

Data information: The bar graphs (mean ± SEM) display pooled data from two to four (A) or three (G) independent experiments. Total number of cells analysed in (A) are as follows: FL-HTT: $n = 51$; N586HTT+C-HTT587: $n = 109$; N167HTT+C-HTT587: $n = 95$. Statistics were done by one-way ANOVA with Bonferroni's multiple comparison tests (A) and one-way ANOVA with unpaired *t*-test (G). **$P < 0.01$, ***$P < 0.001$. See also Fig EV3.
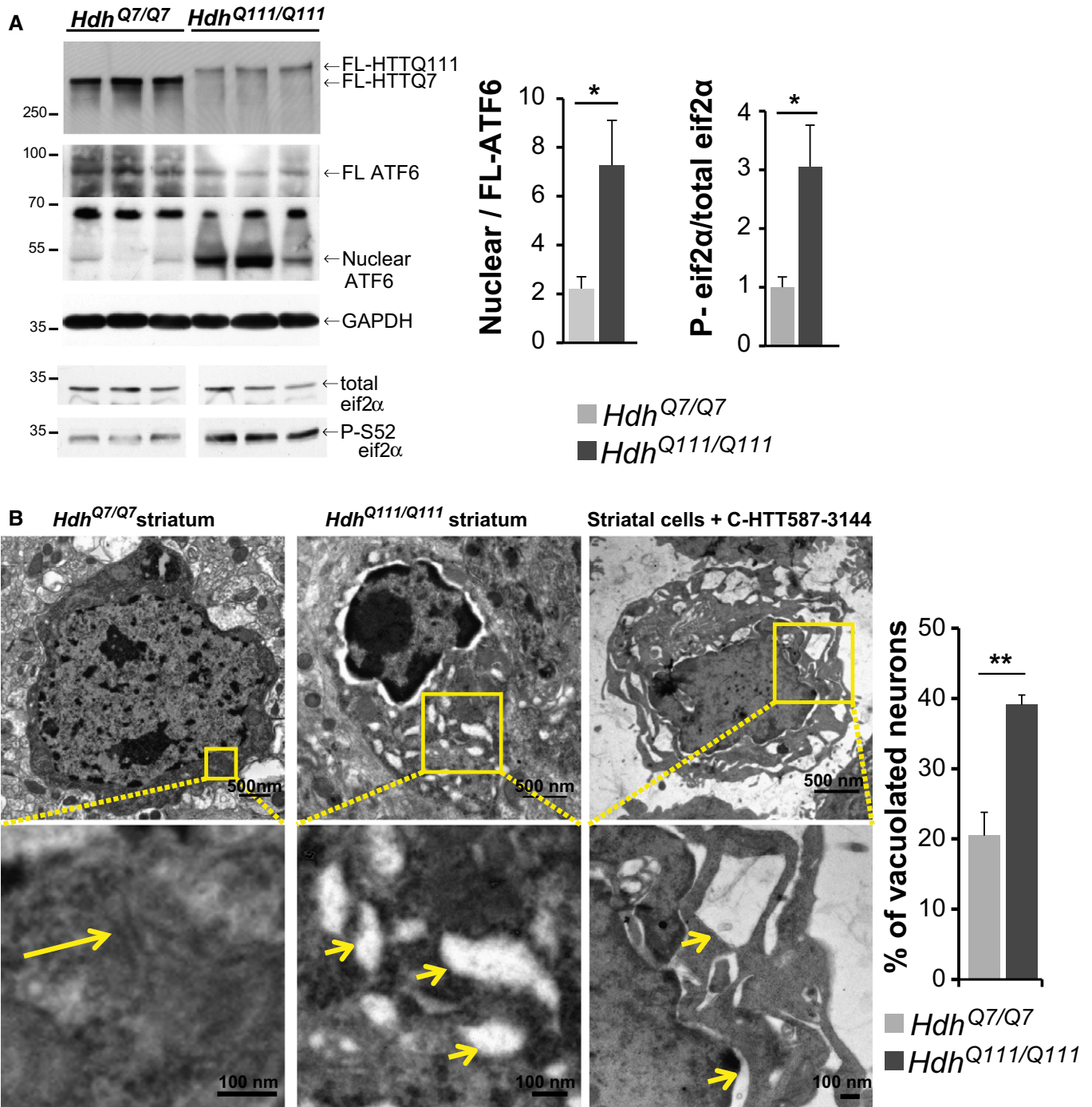
Figure 4. ER stress and vacuolation in HD mouse model.

A   Activation of ER stress in $Hdh^{Q111/Q111}$ knock-in HD mouse model compared to wild-type $Hdh^{Q7/Q7}$ mice.

B   Electron microscopy analysis of striatal sections from 20-month-old $Hdh^{Q7/Q7}$ (left), $Hdh^{Q111/Q111}$ mice (middle) and striatal cells expressing the C-HTT587-3144 construct (right). The long arrow indicates ER, and the small ones depict vacuolated ER.

Data information: The bar graphs (mean ± SEM) display pooled data from 6 to 8 mice of 20 months of age of each genotype (A) and from three mice (B). In (B), total number of neurons analysed are as follows: $Hdh^{Q7/Q7}$ mice: 225; $Hdh^{Q111/Q111}$: 233. Statistics were done by one-way ANOVA with unpaired *t*-test (B, $P = 0.0068$). *$P < 0.05$, **$P < 0.01$.

construct (Fig 5A, left panel). Crossing these flies with UAS-TEV flies led to selective cleavage of HTT *in vivo* (Fig 5A, right panel). Flies expressing the various FL-HTTQ200 constructs without TEV

showed similar deficits in their climbing activity (Fig 5B, left graph). Upon TEV induction, only double proteolysis of HTT significantly decreased the climbing activity of the flies (Fig 5B, right graph).
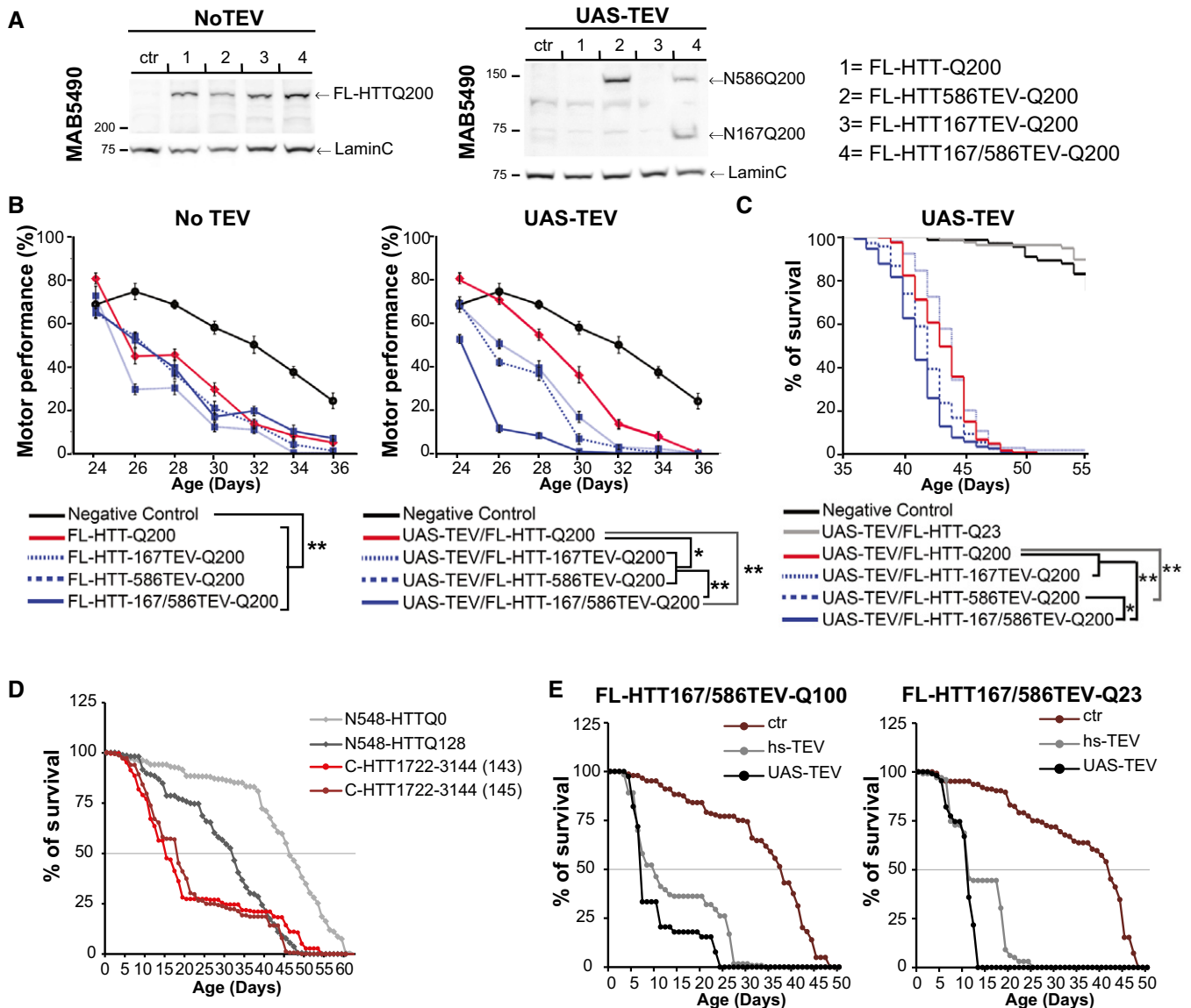
Figure 5. Sequential proteolysis of huntingtin causes toxicity *in vivo*.

A   Expression analysis of FL-HTT-TEV-Q200 in *Drosophila*.

B   Charts showing motor performance in climbing tests as a function of age.

C–E   Kaplan–Meier chart depicts survivorship in flies. Expression of the TEV was under an UAS or heat-shock (hs) promoter.

Data information: The graphs (mean ± SEM) display pooled data from two replicates of 30 female virgins for each genotype (B, C), from three independent crosses (D, E). Total number of flies are as follows: N548-HTTQ0: 440, N548-HTTQ128: 478, C-HTT1722–3144 (143): 223, C-HTT1722–3144 (145)=223 (D) and FL-HTT167/586TEVQ100: ctr: 144, hs-TEV=119, UAS-TEV: 39; FL-HTT167/586TEVQ23: ctr: 124, hs-TEV: 99, UAS-TEV: 106 (E). Statistics were done by Z-test, *P*-values comparing the slope of decline in motor performance, **$P < 0.00001$, *$P = 0.006756$ (B), or were done by Kaplan–Meier, log-rank significance test (C–E). (C) FL-HTT-Q200 vs FL-HTT167TEV-Q200: ns, FL-HTT-Q200 vs FL-HTT586TEV-Q200: **$P < 0.0001$, FL-HTT-Q200 vs FL-HTT167/586TEV-Q200: **$P < 0.0001$, FL-HTT586TEV-Q200 vs FL-HTT167/586TEV-Q200: *$P < 0.0069$. (D) N548-HTTQ0 vs N548-HTTQ128: $P < 0.001$, C-HTT1722–3144 (143) & (145) vs N548-HTTQ128: $P < 0.01$. (E) pcDNA vs TEV: $P < 0.001$. See also Fig EV4.

Similarly, and as observed in cells, double HTT proteolysis was significantly more toxic to flies than any other combinations (Fig 5C).

We investigated whether the C-ter fragment alone was sufficient to alter fly survival *in vivo*. We failed to generate transgenic flies expressing the C-HTT587-3144 fragment, so we used a shorter C-terminal fragment: C-HTT1722–3144. This fragment interacts with

the N586 fragment but not with the N167 fragment and, when expressed in cells, leads to vacuolation and death (Fig EV4A). N548-HTTQ128 flies showed a decreased survival rate compared to flies expressing wild-type N548-HTTQ0 (Lee *et al*, 2004). C-HTT1722–3144 flies had even a shorter lifespan (Fig 5D) as shown in two independent lines (143 & 145). It is unlikely that the toxicity was due to overexpression as the C-HTT1722–3144

fragment was detected only by immunoprecipitation, whereas the N548-HTT fragments were readily detected directly in whole fly brain extracts (Fig EV4B and C).

Thus, both N-ter and C-ter products of polyQ FL-HTT proteolysis are toxic *in vivo*. Finally, we generated transgenic flies expressing the TEV protease constructs and FL-HTT containing two TEV sites and with either 100Q or 23Q with expression driven by Elav-Gal4. TEV expression led to a dramatic reduction in fly survival both for the polyQ-containing ones and for wild-type flies. Similar results were obtained in experiments with TEV expression under the control of the heat-shock promoter, hs-TEV (Pauli *et al*, 2008), or of the UAS-TEV (Fig 5E).

Dynamin 1 interacts with the C-terminal part of huntingtin

To decipher the mechanism by which the C-HTT587-3144 fragment leads to ER vacuolation, we searched for proteins interacting with the C-terminal domain of HTT. However, most reported yeast two-hybrid screens have been performed using N-terminal fragments of HTT, and the ones performed with C-terminal fragments as baits did not identify any specific interactors (Faber *et al*, 1998; Kaltenbach *et al*, 2007).

To optimise the strategy for identifying potential C-terminal HTT interactors, we searched the primary sequences of HTT orthologues for highly conserved regions. We found a fragment from position 1230 to position 3144 that shows a substantial similarity between the various species (Fig EV5A and B) and used it as bait for a yeast two-hybrid screen using an adult human brain library. We obtained four interactors with high confidence (Fig 6A) including dynamin 1. Dynamin 1 is involved in membrane fission reactions during several cellular processes (Ferguson & De Camilli, 2012) and has been identified as an interactor with the HTT N-terminal region (Kaltenbach *et al*, 2007) and full-length HTT (Moreira Sousa *et al*, 2013). Therefore, dynamin 1 may interact with both the N-ter and C-ter domains of full-length HTT, and proteolysis may affect the interaction between dynamin 1 and HTT. To test this possibility, we SNIPer-TEV-cleaved HTT at position 586 or at both positions 167 and 586 and immunoprecipitated HTT N-ter. FL-HTT and the N586 fragment interacted with dynamin 1, but the N167 fragment produced after the double cleavage did not (Fig 6B). We also found that FL-HTT, C-HTT587-3144 and N586-HTTQ100, but not the shorter N167-HTTQ100 fragment, interacted with dynamin 1 (Fig 6C). We conclude that the interaction between HTT and dynamin 1 may be affected by sequential proteolysis of N-ter fragments.

Dynamin 1 and huntingtin localise at ER membranes

Although dynamin 1 has not been described at the ER, dynamin-like proteins, including atlastin/Sey1p and Lnp1p, are enriched at the ER where they mediate its fusion/fission (Hu *et al*, 2009; Orso *et al*, 2009; Chen *et al*, 2013). Fractionation of both wild-type (STHdhQ7/Q7)- and mutant (STHdhQ111/Q111)-immortalised striatal cell line samples and of mouse brains revealed the presence of dynamin 1 in the enriched ER membrane fractions (Fig 6D). ER-enriched fractions did not show the presence of cytosolic proteins such as tubulin, plasma membrane proteins such as annexin V, nor mitochondrial proteins such as the mitochondrial protein hsp70. ER fraction was slightly contaminated with the endosomal marker EEA1 and TGN138. However, it exhibited a large enrichment in the ER membrane protein calnexin (Fig 6D). We next used direct STochastic Optical Reconstruction Microscopy (dSTORM) to localise endogenous dynamin 1 and calnexin in cells: Alexa 568 was used as the photoswitchable fluorophore and revealed that both proteins had a tubulo-membranous organisation (Fig 6E, top panels). Co-immunostaining revealed dynamin 1 on ER structures identified by calnexin staining (Fig 6E, lower panels). Finally, we transfected striatal cells with a construct encoding dynamin 1-GFP and performed immuno-electron microscopy. There were significantly more gold particles at ER membranes in cells transfected with the dynamin 1-GFP construct than those transfected with the GFP vector (Fig 6F). These various analyses demonstrate that dynamin 1 can be found at ER membranes.

We also analysed the localisation of various HTT fragments. Subcellular fractionation identified FL-HTT and all the various HTT fragments in the ER-enriched fraction and, possibly, accumulation of the C-HTT587-3144 fragment in this fraction (Fig 6G). This confirms previous reports that full-length HTT localises at the ER (Atwal *et al*, 2007) and shows that the C-HTT587-3144 fragment resulting from HTT sequential N-terminal proteolysis remains at the ER co-localising with dynamin 1.

Dynamin 1 impairment at the ER mediates the effect of C-ter huntingtin on vacuolation and death

We next investigated whether dynamin 1 influenced C-HTT587-3144 fragment-associated vacuolation and death. The toxicity associated with the presence of the C-HTT587-3144 fragment was significantly reduced by the co-expression of WT-dynamin 1 (Fig 6H); similarly, the percentage of vacuolated cells was significantly reduced. These findings suggest that C-HTT587-3144

Figure 6.　Dynamin 1 interacts with C-terminal huntingtin and both associate to ER membranes.

A　Schematic representation of the bait used in the yeast two-hybrid screen and list of the four confident interactors with their HTT-interacting domains.

B, C　HeLa cells expressing HTT-TEV (B) or HTT fragments (C) with dynamin 1 were subjected to immunoprecipitation and immunoblotting analyses.

D　Cellular fractionation analysis of striatal cells or *Hdh* mice model. Total (T), cytosolic (C) and ER membrane (E) fractions.

E　Localisation of dynamin 1 at ER membranes (calnexin immunostaining) using dSTORM method in striatal cells.

F　Immuno-electron microscopy analyses of dynamin 1 at ER in striatal cells. Enlargement indicates an ER tubule.

G　Cellular fractionation and ER localisation of HTT fragments expressed in striatal cells.

H　Cell death (left) and vacuolation (right) analysis in C-HTT587-3144 cells co-expressing WT-dynamin 1 in striatal cells.

Data information: The bar graphs (mean ± SEM) display pooled data from 80 isolated ER tubules in empty GFP-expressing cells and 140 in dynamin 1-GFP-expressing cells (F) or from 6 independent experiments in triplicate (H). Statistics were done by one-way ANOVA, unpaired *t*-test, **P = 0.0015 (F) and by one-way ANOVA with Bonferroni's multiple comparison test, ***P < 0.001 (H). See also Fig EV5.
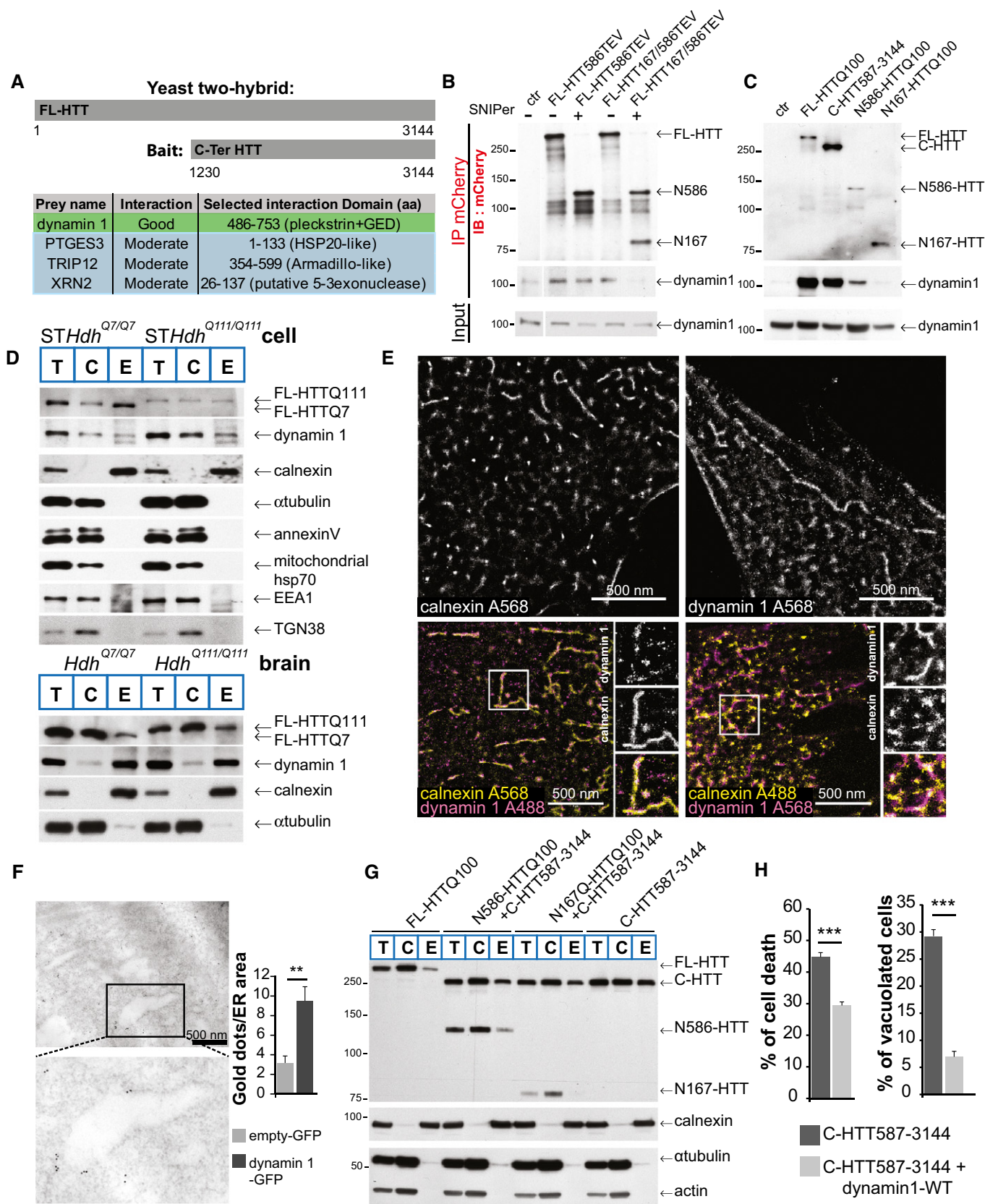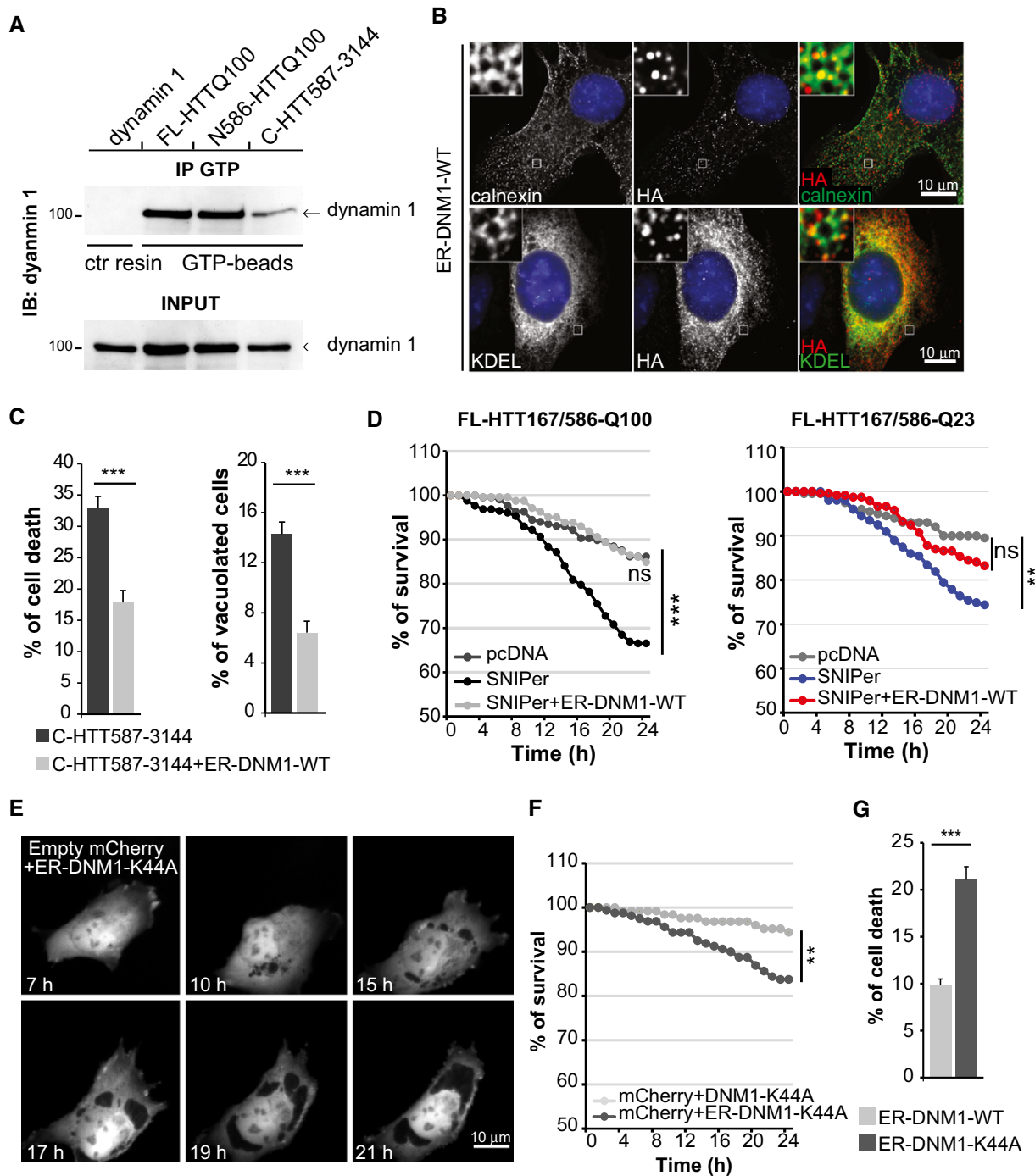
Figure 6.

Figure 7. C-terminal huntingtin impairs the activity of ER-localised dynamin 1 that subsequently induces ER dilation and death.

A   GTP-bound dynamin 1 levels were analysed in ER-enriched membranes from HEK293T cells expressing the indicated HTT constructs.

B   Immunostaining of engineered artificially ER-targeted DNM1-WT (anti-HA) and ER network (calnexin and GFP-KDEL markers) expressed in striatal cells.

C   Analysis of toxicity and vacuolation of striatal cells expressing C-HTT587-3144 fragment and ER-DNM1-WT.

D   Survival curves upon cleavage of FL-HTT167/586TEV co-expressing ER-DNM1-WT in striatal cells.

E   Time-lapse analysis by fluorescence live microscopy of striatal cells co-expressing an empty mCherry vector with ER-DNM1-K44A vector.

F   Survival curves of striatal cells expressing empty mCherry vector and DNM1-K44A or ER-DNM1-K44A.

G   Quantification of cell death induced by ER-targeted wild-type and mutant dynamin 1 in striatal cells

Data information: The graphs (mean ± SEM) display pooled data from three independent experiments. The total number of cells assessed are as follows: (D) FL-HTT167/586TEV+pcDNA: 192 or +SNIPer: 238; FL-HTT167/586-Q100 + ER-DNM1-WT: pcDNA: 272 or + SNIPer: 245; FL-HTT167/586TEV+pcDNA: 200 or + SNIPer: 199; FL-HTT167/586-Q23 + ER-DNM1-WT: pcDNA: 270 or + SNIPer: 239 and (F) DNM1-DN: 125, ER-DNM1-DN: 160. Statistics were done by unpaired *t*-test (C), log-rank test (D, F) or one-way ANOVA with unpaired *t*-test (G). ns: non-significant, **$P < 0.01$, ***$P < 0.001$. See also Fig EV5.

fragment-induced vacuolation and death involve deregulation of dynamin 1 activity.

The role of dynamin 1 in endocytosis has been clearly established. We measured transferrin uptake in striatal cells containing the C-HTT587-3144 fragment and found a lower endocytic rate than control values (Fig EV5C); this effect was abolished by the expression of WT-dynamin 1. Oligomerisation of dynamin 1 is required for GTPase activity (Zhang *et al*, 2012); using a crosslinking approach, we found that dynamin 1 oligomerisation was reduced by the presence of the C-HTT587-3144 fragment (Fig EV5D). To measure dynamin 1 activity selectively at the ER, we quantified the GTP-bound form of dynamin 1 at ER membranes purified from HEK293T cells expressing dynamin 1 and various HTT constructs. An anti-GTP immunoprecipitation (Sugiura *et al*, 2013) revealed that GTP-bound dynamin 1 was reduced by 55% ($\pm$ 22%) in cells containing the C-HTT587-3144 fragment compared to those containing the FL-HTTQ100 or N586-HTTQ100 fragment (Fig 7A). These experiments indicate that the C-ter fragment of HTT decreases dynamin 1 activity at both the plasma and ER membranes.

We next tested whether the ER vacuolation associated with HTT proteolysis was due to a defect in the activity of the dynamin 1 localised at the ER. We generated constructs encoding WT or dominant-negative K44A dynamin 1 tagged with an HA sequence at its N-terminus and fused to the transmembrane domain of atlastin 1 at its C-terminus. These fusion proteins, termed ER-DNM1-WT and ER-DNM1-K44A, respectively, were artificially targeted to the ER, as evidenced both by cellular fractionation experiments (Fig EV5E) and co-localisation with calnexin, KDEL-GFP and ER-dsRed markers in striatal cells (Figs 7B and EV5F and G). We then co-expressed ER-DNM1 and various HTT constructs in striatal cells. Consistent with the findings for dynamin 1, a significant fraction of FL-HTTQ100, C-HTT587-3144 and N586-HTTQ100 interacted with ER-DNM1, whereas the shorter N167-HTTQ100 fragment did not (Fig EV5H). These results indicate that both FL-HTT and the proteolytic products generated by cleavage at position 586 interact with dynamin 1 at the ER. However, sequential proteolysis generating small N-ter fragments results in only the C-ter HTT product remaining associated with the ER-localised dynamin 1.

We assessed the consequences of ER-targeted dynamin 1 expression on ER vacuolation and death associated with the C-HTT587-3144 fragment. The percentages of dead cells and vacuolated cells were significantly lower in the presence than absence of ER-DNM1-WT (Fig 7C). We next co-expressed FL-HTT167/586TEV-Q100 and ER-DNM1-WT constructs in the presence of SNIPer-TEV system and treated the cells with 20 nM rapamycin. The toxicity induced by the double proteolysis of HTT was significantly reduced by the expression of the ER-DNM1-WT construct (Fig 7D). Thus, re-establishing dynamin 1 activity at the ER membranes was sufficient to prevent the cell death caused by double cleavage of HTT.

These findings suggest that specifically targeting inactive dynamin 1 to the ER should be sufficient to cause vacuolation and death. Indeed, we found that targeting the DNM1-K44A mutant to the ER caused ER dilation and vacuolation in about 11% of the transfected cells ($n = 160$ cells), whereas no vacuolated cells were observed in cells transfected with the DNM1-K44A mutant not targeted to the ER ($n = 125$ cells) (Figs 7E and EV5G). Similarly, ER-targeted inactive dynamin 1, but not its cytoplasmic form, caused significant cell death (Fig 7F). Also, the inactive ER-DNM1-K44A
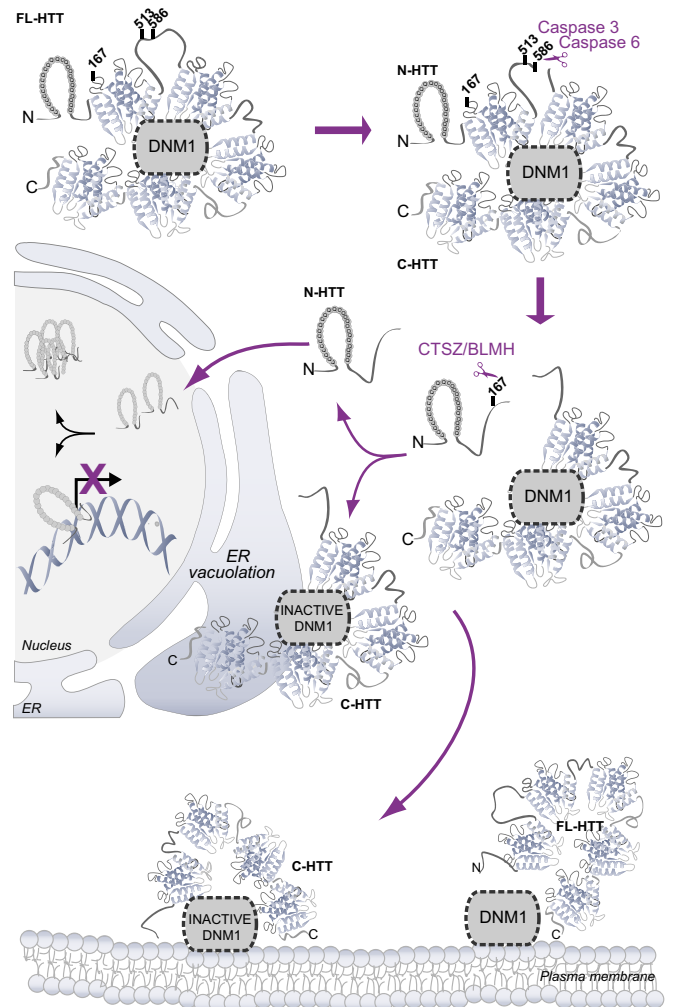

Figure 8. Canonical and non-canonical pathways induced after huntingtin proteolysis.
Cartoon summarising the sequential proteolysis of full-length HTT (FL-HTT) leading to the generation of N-terminal-containing polyQ fragments (N-HTT) that translocate into the nucleus and C-terminal fragments (C-HTT) that localise at the ER and inactivate dynamin 1 (DNM1) leading to ER dilation, ER stress and toxicity. Toxicity may also involve dynamin 1 inhibition on endocytosis, at the plasma membrane.

mutant but not the ER-DNM1-WT constructs were toxic, showing that this effect was specifically due to inactivation of dynamin 1 at ER membranes (Fig 7G) .

Overall, our results indicate that sequential N-terminal proteolysis of HTT generates a C-terminal fragment that inactivates dynamin 1 at plasma and ER membranes. In addition to inhibit endocytosis, HTT C-ter fragment inhibits dynamin 1 at ER membranes that leads to abnormal ER vacuolation and death (Fig 8).

Discussion

Studies that addressed the consequences of HTT proteolysis have either compared the relative toxicities of the various N-ter polyQ fragments generated by proteolysis (Hackam *et al*, 1998) or

expressed point mutants for these sites and analysed the consequences of the absence of cleavage on polyQ-HTT-induced toxicity (Wellington *et al*, 2000; Gafni *et al*, 2004; Graham *et al*, 2006; Miller *et al*, 2010). Some studies have analysed the consequences of protease activation or inhibition on polyQ-mediated toxicity, although this approach has the disadvantage of inducing/inhibiting the cleavage of many substrates in addition to HTT. Moreover, the exact identity of the proteases that cleave major proteolytic sites on HTT remains to be established (Lunkes *et al*, 2002; Gafni *et al*, 2012). Here, we used mutant HTT variants in which TEV cleavage sites have been introduced at various known proteolytic sites to investigate the molecular and cellular consequences of selective HTT cleavage at the targeted sites in a controlled manner. Such strategy has been successfully used to investigate proteolysis by, and thus the role of, executioner caspases 3 and 7 (Gray *et al*, 2010). We show this approach to be particularly useful for the study of proteolysis in HD and possibly other neurodegenerative disorders such as Alzheimer's disease in which specific proteolytic events occur.

When assessing various proteolytic sites in HTT, we found that the site at position 167 was not as efficiently cleaved as the sites at positions 586 or 513. These differences may be due to differences in accessibility: positions 586 and 513 are in disordered and exposed regions of the protein, whereas position 167 is located in the first HEAT repeat of HTT which is composed of antiparallel α-helices and therefore may not be accessible to the TEV protease. The presence of a polyQ stretch in HTT favoured the appearance of the N-167 fragment, suggesting that polyQ expansion—in agreement with the polyQ-HTT conformation being different to the wild-type HTT conformation (Trottier *et al*, 1995)—may render the proteolytic site at position 167 more accessible. Cleavages at positions 586 or 513 also increased the accessibility of the site at position 167, consistent with a proteolytic cascade hypothesis. In addition, this approach allowed us to demonstrate that specific proteolytic events lead to the loss of intramolecular interaction between N-ter and C-ter fragments. Although the TEV strategy provides new approach to study HTT proteolysis and its consequences, further work will be necessary to investigate such cleavages on endogenous HTT. Nevertheless, by examining human post-mortem brain samples, we found that in disease, differential proteolysis of mutant HTT generating small N-ter fragments may release the C-ter HTT fragment from intramolecular interaction.

To our knowledge, few studies have addressed the potential role and/or function of HTT C-ter fragments. One used a *Drosophila* HTT fragment that is more C-terminal than the fragment (positions 586–3144) used in our study (Takano & Gusella, 2002). As in our study, the authors found that this fragment was cytoplasmic. Cell death was not assessed, but it was found that this fragment could act as a regulator of the entry of NF-κB/dorsal into the nucleus. A more recent study investigated the potential function of the C-ter part of HTT and discovered that this region has similarity to yeast Atg11 and as such could play a role as a scaffold for selective autophagy. Interestingly, the described C-ter fragments used in this study were reported to be toxic in primary neurons (Ochaba *et al*, 2014). Although in this and our study some of the toxic effect of the C-ter fragment might be due to overexpression artefacts, we found that the selective proteolysis of full-length mutant polyQ-HTT dramatically increases its toxicity. Even, we found that when wild-type full-length HTT is proteolysed, this turns the non-toxic wild-type HTT into a highly toxic protein.

This further supports our findings that C-ter fragments when released from full-length HTT might have some toxicity.

Here we showed that C-ter HTT is toxic in the cytoplasmic compartment by inactivating dynamin 1 at ER membranes leading to ER dilation, ER stress and cell death. We also observed that the C-ter fragment decreases endocytosis as shown by the reduction in transferrin uptake in cells expressing this fragment. The function of dynamin 1 is associated with endocytosis, and to our knowledge, no ER abnormalities in mice deleted for dynamin genes have been reported (Ferguson & De Camilli, 2012). In addition, dynamin inhibition either by dynasore or by the (non-targeted) expression of the dominant-negative dynamin 1 K44A shows no ER-derived phenomena. Nevertheless, using EM, high-resolution detection techniques and biochemical approaches, we reveal that a fraction of dynamin 1 interacts and co-localises with HTT at ER membranes. We also found that selective inactivation of dynamin 1 at the ER promotes ER dilation. Importantly, this functional defect was only observed when dominant-negative dynamin 1 was targeted to the ER or in the presence of the HTT C-ter fragment. Therefore, although we cannot exclude that part of C-ter HTT fragment-induced toxicity could be mediated by the inhibition of endocytosis, the inactivation of dynamin 1 on ER membranes may occur specifically in response to abnormal proteolysis of mutant HTT that is only observed during HD pathogenesis. In support, mutant HTT was shown to disrupt ER morphology leading to the accumulation of clear cytoplasmic vacuoles in striatal immortalised cell lines (Trettel *et al*, 2000), in the brain of knock-in mice (Fig 4), in lymphoblasts from patients with HD (Nagata *et al*, 2004) and in iPSC from patients with HD (Juopperi *et al*, 2012). So it is plausible that a HTT–dynamin 1 complex regulates ER shaping/dynamics and that this complex, if altered in disease, could lead to the formation of cytoplasmic vacuoles. Our findings justify further studies to elucidate the role of this complex at the ER.

Other HTT interactors that bind through the C-ter part of HTT have been identified, but they are unlikely to be linked to the described mechanism since some of them are either co-repressor of transcription or regulate endosomal trafficking (Kegel *et al*, 2002; Pal *et al*, 2006). Recently, bioinformatic and functional analyses revealed that the C-ter fragment shares structural similarity to yeast Atg11. Atg11 is a receptor for the yeast dynamin 1 and promotes the fission of mitochondria and membranes of the ER (Cebollero *et al*, 2012; Mao *et al*, 2013). This further supports the possibility of a role for HTT in the regulation of ER membrane dynamics.

Huntingtin C-ter region may thus have several functions that have been underestimated. As stated previously, yeast two-hybrid screening experiments using HTT C-ter fragments as baits failed to identify any proteins interacting with HTT (Faber *et al*, 1998; Kaltenbach *et al*, 2007). Even by using a large region including HEAT repeats, we only found a small number of proteins interacting with the C-ter of HTT. Coherent with the intramolecular interaction observed (Li *et al*, 2006; Palidwor *et al*, 2009)(this study), HTT may adopt a closed conformation establishing only limited interactions between the C-ter region and other proteins. Nevertheless, our findings and the study by Ochaba and colleagues (Ochaba *et al*, 2014) provide evidence that the C-ter region of HTT has an important role in regulating HTT function and toxicity in health and disease.

Our study reveals that HTT proteolysis, in addition to generate small N-ter fragments that are toxic in the nucleus, releases

non-polyQ C-ter fragments that may also be relevant to HD pathogenesis. Determining the physiological relevance of such fragments in disease may lead to new therapeutic strategies.

Materials and Methods

Mice

Mice are Hdh^{Q111} HD knock-in mouse model (Wheeler *et al*, 1999). Experimental procedures were performed in accordance with the recommendations of the European Community (86/609/EEC) and the French National Committee (2010/63) for care and use of laboratory animals. See Appendix Supplementary Materials and Methods for further details.

Flies

FL-HTT-Q100 transgenic flies were generated by Bestgene, Inc. FL-HTT-Q200 flies were generated through subcloning of FL-HTT constructs into P[acman] and subsequent site-directed insertion using the PhiC31 integrase. Survival, climbing assay and brain structure analyses were performed on various HTT constructs expressing flies. Fly strains, crosses and analyses are described in Appendix Supplementary Materials and Methods.

Constructs

The FL-HTT-TEV constructs encode the human HTT protein containing a TEV recognition cleavage sites (TEVrcs) at specific positions. Amino acids corresponding to the endogenous cleavage sites of caspase-6 (D586), caspase-3 (D510SVDL514) and cathepsin Z/bleomycin hydrolase (R167) were replaced by the recognition cleavage site (rcs) of the TEV protease: ENLYFQS. ER-DNM1-WT and ER-DNM1-K44A constructs encode for dynamin 1-WT (DNM1-WT) or mutant K44A (DNM1-K44A), respectively, targeted to endoplasmic reticulum membranes by fusion to the endoplasmic reticulum transmembrane domain of atlastin 1. Further details on the generation of constructs are provided in Appendix Supplementary Materials and Methods.

Proteolysis of huntingtin-TEV constructs

For *in vitro* cleavage of HTT by recombinant TEV protease, cells were transfected with the FL-HTT-TEV and extracts were incubated with recombinant TEV protease. For intracellular HTT cleavage, cells were co-transfected with the FL-HTT-TEV constructs and the SNIPer-TEV plasmids or pcDNA for control conditions and treated with rapamycin.

Videomicroscopy, immunoelectron and super-resolution microscopies

For videomicroscopy, striatal cells were electroporated with fluorescent-tagged constructs and subsequently analysed by time-lapse multi-position videomicroscopy following individual transfected cells up to 24 h. Dynamics of individual cells were analysed to establish the kinetics of vacuolation and death upon various conditions and specific markers. For electron and light microscopy, cells or tissues were fixed and subjected to Epon embedding prior to sectioning. For immunoelectron microscopy, cells were fixed and stained with immunogold particles and uranyl acetate. For super-resolution microscopy, we used direct STochastic Optical Reconstruction Microscopy (dSTORM) on cells to analyse the localisation of dynamin 1 with the ER marker calnexin. Further details are provided in Appendix Supplementary Materials and Methods.

Endoplasmic reticulum isolation and dynamin 1 activity

ER membranes were purified through successive subcellular fractionation and sucrose gradient fractionation. Dynamin 1 activity was assessed by transferrin uptake measured on cell-sorted cells, measurement of the GTP binding of dynamin 1 on GTP-coupled beads and of the membrane-associated dynamin 1 through cross-linking of dynamin 1 using a non-cleavable and membrane permeable cross-linker DSS. Further details are provided in Appendix Supplementary Materials and Methods.

Expanded view for this article is available online:
http://emboj.embopress.org

Author contributions

M-TE-D and EH conceived, designed and carried out experiments, analysed the data and wrote a draft of the manuscript. JB performed Golgi reassembly assays and the post-mortem brain analyses. RP did the first toxicity experiments with C-ter fragments and designed the Y2H. GP generated most of the constructs used in the study and helped throughout the study, IA-R generated and analysed the FL-HTT-Q23 and Q200 flies under JB supervision, NB, CM and SL-F developed and analysed dynamin 1 localisation by dSTORM, and SS and GPi performed the electronic microscopy. FS and SH conceived the project with M-TE-D, and EH helped interpret the data and wrote the manuscript.

Conflict of interest

The authors declare that they have no conflict of interest.

References

Atwal RS, Xia J, Pinchev D, Taylor J, Epand RM, Truant R (2007) Huntingtin has a membrane association signal that can modulate huntingtin aggregation, nuclear entry and toxicity. *Hum Mol Genet* 16: 2600–2615

Borrell-Pages M, Zala D, Humbert S, Saudou F (2006) Huntington's disease: from huntingtin function and dysfunction to therapeutic strategies. *Cell Mol Life Sci* 63: 2642–2660

Cattaneo E, Zuccato C, Tartari M (2005) Normal huntingtin function: an alternative approach to Huntington's disease. *Nat Rev Neurosci* 6: 919–930

Caviston JP, Ross JL, Antony SM, Tokito M, Holzbaur EL (2007) Huntingtin facilitates dynein/dynactin-mediated vesicle transport. *Proc Natl Acad Sci USA* 104: 10045–10050

Cebollero E, Reggiori F, Kraft C (2012) Reticulophagy and ribophagy: regulated degradation of protein production factories. *Int J Cell Biol* 2012: 182834

Chen S, Novick P, Ferro-Novick S (2013) ER structure and function. *Curr Opin Cell Biol* 25: 428–433

Faber PW, Barnes GT, Srinidhi J, Chen J, Gusella JF, MacDonald ME (1998) Huntingtin interacts with a family of WW domain proteins. *Hum Mol Genet* 7: 1463–1474

Ferguson SM, De Camilli P (2012) Dynamin, a membrane-remodelling GTPase. *Nat Rev Mol Cell Biol* 13: 75–88

Gafni J, Ellerby LM (2002) Calpain activation in Huntington's disease. *J Neurosci* 22: 4842–4849

Gafni J, Hermel E, Young JE, Wellington CL, Hayden MR, Ellerby LM (2004) Inhibition of calpain cleavage of huntingtin reduces toxicity: accumulation of calpain/caspase fragments in the nucleus. *J Biol Chem* 279: 20211–20220

Gafni J, Papanikolaou T, Degiacomo F, Holcomb J, Chen S, Menalled L, Kudwa A, Fitzpatrick J, Miller S, Ramboz S, Tuunanen PI, Lehtimaki KK, Yang XW, Park L, Kwak S, Howland D, Park H, Ellerby LM (2012) Caspase-6 activity in a BACHD mouse modulates steady-state levels of mutant huntingtin protein but is not necessary for production of a 586 amino acid proteolytic fragment. *J Neurosci* 32: 7454–7465

Godin JD, Colombo K, Molina-Calavita M, Keryer G, Zala D, Charrin BC, Dietrich P, Volvert ML, Guillemot F, Dragatsis I, Bellaiche Y, Saudou F, Nguyen L, Humbert S (2010) Huntingtin is required for mitotic spindle orientation and mammalian neurogenesis. *Neuron* 67: 392–406

Goldberg YP, Nicholson DW, Rasper DM, Kalchman MA, Koide HB, Graham RK, Bromm M, Kazemi-Esfarjani P, Thornberry NA, Vaillancourt JP, Hayden MR (1996) Cleavage of huntingtin by apopain, a proapoptotic cysteine protease, is modulated by the polyglutamine tract. *Nat Genet* 13: 442–449

Graham RK, Deng Y, Slow EJ, Haigh B, Bissada N, Lu G, Pearson J, Shehadeh J, Bertram L, Murphy Z, Warby SC, Doty CN, Roy S, Wellington CL, Leavitt BR, Raymond LA, Nicholson DW, Hayden MR (2006) Cleavage at the caspase-6 site is required for neuronal dysfunction and degeneration due to mutant huntingtin. *Cell* 125: 1179–1191

Gray DC, Mahrus S, Wells JA (2010) Activation of specific apoptotic caspases with an engineered small-molecule-activated protease. *Cell* 142: 637–646

Hackam AS, Singaraja R, Wellington CL, Metzler M, McCutcheon K, Zhang T, Kalchman M, Hayden MR (1998) The influence of huntingtin protein size on nuclear localisation and cellular toxicity. *J Cell Biol* 141: 1097–1105

Harder B, Schomburg A, Pflanz R, Kustner K, Gerlach N, Schuh R (2008) TEV protease-mediated cleavage in Drosophila as a tool to analyse protein functions in living organisms. *Biotechniques* 44: 765–772

Hermel E, Gafni J, Propp SS, Leavitt BR, Wellington CL, Young JE, Hackam AS, Logvinova AV, Peel AL, Chen SF, Hook V, Singaraja R, Krajewski S, Goldsmith PC, Ellerby HM, Hayden MR, Bredesen DE, Ellerby LM (2004) Specific caspase interactions and amplification are involved in selective neuronal vulnerability in Huntington's disease. *Cell Death Differ* 11: 424–438

Hu J, Shibata Y, Zhu PP, Voss C, Rismanchi N, Prinz WA, Rapoport TA, Blackstone C (2009) A class of dynamin-like GTPases involved in the generation of the tubular ER network. *Cell* 138: 549–561

Imarisio S, Carmichael J, Korolchuk V, Chen CW, Saiki S, Rose C, Krishna G, Davies JE, Ttofi E, Underwood BR, Rubinsztein DC (2008) Huntington's disease: from pathology and genetics to potential therapies. *Biochem J* 412: 191–209

Juopperi TA, Kim WR, Chiang CH, Yu H, Margolis RL, Ross CA, Ming GL, Song H (2012) Astrocytes generated from patient induced pluripotent stem cells recapitulate features of Huntington's disease patient cells. *Mol Brain* 5: 17

Kaltenbach LS, Romero E, Becklin RR, Chettier R, Bell R, Phansalkar A, Strand A, Torcassi C, Savage J, Hurlburt A, Cha GH, Ukani L, Chepanoske CL, Zhen Y, Sahasrabudhe S, Olson J, Kurschner C, Ellerby LM, Peltier JM, Botas J et al (2007) Huntingtin interacting proteins are genetic modifiers of neurodegeneration. *PLoS Genet* 3: e82

Kegel KB, Meloni AR, Yi Y, Kim YJ, Doyle E, Cuiffo BG, Sapp E, Wang Y, Qin ZH, Chen JD, Nevins JR, Aronin N, DiFiglia M (2002) Huntingtin is present in the nucleus, interacts with the transcriptional corepressor C-terminal binding protein, and represses transcription. *J Biol Chem* 277: 7466–7476

Kim YJ, Sapp E, Cuiffo BG, Sobin L, Yoder J, Kegel KB, Qin ZH, Detloff P, Aronin N, DiFiglia M (2006) Lysosomal proteases are involved in generation of N-terminal huntingtin fragments. *Neurobiol Dis* 22: 346–356

Kim YJ, Yi Y, Sapp E, Wang Y, Cuiffo B, Kegel KB, Qin ZH, Aronin N, DiFiglia M (2001) Caspase 3-cleaved N-terminal fragments of wild-type and mutant huntingtin are present in normal and Huntington's disease brains, associate with membranes, and undergo calpain-dependent proteolysis. *Proc Natl Acad Sci USA* 98: 12784–12789

Landles C, Bates GP (2004) Huntingtin and the molecular pathogenesis of Huntington's disease. Fourth in molecular medicine review series. *EMBO Rep* 5: 958–963

Landles C, Sathasivam K, Weiss A, Woodman B, Moffitt H, Finkbeiner S, Sun B, Gafni J, Ellerby LM, Trottier Y, Richards WG, Osmand A, Paganetti P, Bates GP (2010) Proteolysis of mutant huntingtin produces an exon 1 fragment that accumulates as an aggregated protein in neuronal nuclei in Huntington disease. *J Biol Chem* 285: 8808–8823

Lee WC, Yoshihara M, Littleton JT (2004) Cytoplasmic aggregates trap polyglutamine-containing proteins and block axonal transport in a Drosophila model of Huntington's disease. *Proc Natl Acad Sci USA* 101: 3224–3229

Li W, Serpell LC, Carter WJ, Rubinsztein DC, Huntington JA (2006) Expression and characterization of full-length human huntingtin, an elongated HEAT repeat protein. *J Biol Chem* 281: 15916–15922

Li XJ, Li S (2010) Proteasomal dysfunction in aging and Huntington disease. *Neurobiol Dis* 43: 4–8

Lunkes A, Lindenberg KS, Ben-Haiem L, Weber C, Devys D, Landwehrmeyer GB, Mandel JL, Trottier Y (2002) Proteases acting on mutant huntingtin generate cleaved products that differentially build up cytoplasmic and nuclear inclusions. *Mol Cell* 10: 259–269

Mangiarini L, Sathasivam K, Seller M, Cozens B, Harper A, Hetherington C, Lawton M, Trottier Y, Lehrach H, Davies SW, Bates GP (1996) Exon 1 of the HD gene with an expanded CAG repeat is sufficient to cause a progressive neurological phenotype in transgenic mice. *Cell* 87: 493–506

Mao K, Wang K, Liu X, Klionsky DJ (2013) The scaffold protein Atg11 recruits fission machinery to drive selective mitochondria degradation by autophagy. *Dev Cell* 26: 9–18

Mende-Mueller LM, Toneff T, Hwang SR, Chesselet MF, Hook VY (2001) Tissue-specific proteolysis of Huntingtin (htt) in human brain: evidence of enhanced levels of N- and C-terminal htt fragments in Huntington's disease striatum. *J Neurosci* 21: 1830–1837

Miller JP, Holcomb J, Al-Ramahi I, de Haro M, Gafni J, Zhang N, Kim E, Sanhueza M, Torcassi C, Kwak S, Botas J, Hughes RE, Ellerby LM (2010) Matrix metalloproteinases are modifiers of huntingtin proteolysis and toxicity in Huntington's disease. *Neuron* 67: 199–212

Moreira Sousa C, McGuire JR, Thion MS, Gentien D, de la Grange P, Tezenas du Montcel S, Vincent-Salomon A, Durr A, Humbert S (2013) The Huntington disease protein accelerates breast tumour development and metastasis through ErbB2/HER2 signalling. *EMBO Mol Med* 5: 309–325

Nagata E, Sawa A, Ross CA, Snyder SH (2004) Autophagosome-like vacuole formation in Huntington's disease lymphoblasts. *NeuroReport* 15: 1325–1328

Ochaba J, Lukacsovich T, Csikos G, Zheng S, Margulis J, Salazar L, Mao K, Lau AL, Yeung SY, Humbert S, Saudou F, Klionsky DJ, Finkbeiner S, Zeitlin SO, Marsh JL, Housman DE, Thompson LM, Steffan JS (2014) Potential function for the Huntingtin protein as a scaffold for selective autophagy. *Proc Natl Acad Sci USA* 111: 16889–16894

Orso G, Pendin D, Liu S, Tosetto J, Moss TJ, Faust JE, Micaroni M, Egorova A, Martinuzzi A, McNew JA, Daga A (2009) Homotypic fusion of ER membranes requires the dynamin-like GTPase atlastin. *Nature* 460: 978–983

Pal A, Severin F, Lommer B, Shevchenko A, Zerial M (2006) Huntingtin-HAP40 complex is a novel Rab5 effector that regulates early endosome motility and is up-regulated in Huntington's disease. *J Cell Biol* 172: 605–618

Palidwor GA, Shcherbinin S, Huska MR, Rasko T, Stelzl U, Arumughan A, Foulle R, Porras P, Sanchez-Pulido L, Wanker EE, Andrade-Navarro MA (2009) Detection of alpha-rod protein repeats using a neural network and application to huntingtin. *PLoS Comput Biol* 5: e1000304

Pardo R, Molina-Calavita M, Poizat G, Keryer G, Humbert S, Saudou F (2010) pARIS-htt: an optimised expression platform to study huntingtin reveals functional domains required for vesicular trafficking. *Mol Brain* 3: 17

Pauli A, Althoff F, Oliveira RA, Heidmann S, Schuldiner O, Lehner CF, Dickson BJ, Nasmyth K (2008) Cell-type-specific TEV protease cleavage reveals cohesin functions in Drosophila neurons. *Dev Cell* 14: 239–251

Ratovitski T, Chighladze E, Waldron E, Hirschhorn RR, Ross CA (2011) Cysteine proteases bleomycin hydrolase and cathepsin Z mediate N-terminal proteolysis and toxicity of mutant huntingtin. *J Biol Chem* 286: 12578–12589

Ratovitski T, Gucek M, Jiang H, Chighladze E, Waldron E, D'Ambola J, Hou Z, Liang Y, Poirier MA, Hirschhorn RR, Graham R, Hayden MR, Cole RN, Ross CA (2009) Mutant huntingtin N-terminal fragments of specific size mediate aggregation and toxicity in neuronal cells. *J Biol Chem* 284: 10855–10867

Romero E, Cha GH, Verstreken P, Ly CV, Hughes RE, Bellen HJ, Botas J (2008) Suppression of neurodegeneration and increased neurotransmission caused by expanded full-length huntingtin accumulating in the cytoplasm. *Neuron* 57: 27–40

Sathasivam K, Neueder A, Gipson TA, Landles C, Benjamin AC, Bondulich MK, Smith DL, Faull RL, Roos RA, Howland D, Detloff PJ, Housman DE, Bates GP (2013) Aberrant splicing of HTT generates the pathogenic exon 1 protein in Huntington disease. *Proc Natl Acad Sci USA* 110: 2366–2370

Saudou F, Finkbeiner S, Devys D, Greenberg ME (1998) Huntingtin acts in the nucleus to induce apoptosis but death does not correlate with the formation of intranuclear inclusions. *Cell* 95: 55–66

Sugars KL, Rubinsztein DC (2003) Transcriptional abnormalities in Huntington's disease. *Trends Genet* 19: 233–238

Sugiura A, Nagashima S, Tokuyama T, Amo T, Matsuki J, Ishido S, Kudo Y, McBride HM, Fukuda T, Matsushita N, Inatome R, Yanagi S (2013) MITOL regulates endoplasmic reticulum-mitochondria contacts via Mitofusin 2. *Mol Cell* 51: 20–34

Takano H, Gusella JF (2002) The predominantly HEAT-like motif structure of huntingtin and its association and coincident nuclear entry with dorsal, an NF-kB/Rel/dorsal family transcription factor. *BMC Neurosci* 3: 15

Tebbenkamp AT, Crosby KW, Siemienski ZB, Brown HH, Golde TE, Borchelt DR (2012) Analysis of Proteolytic Processes and Enzymatic Activities in the Generation of Huntington N-Terminal Fragments in an HEK293 Cell Model. *PLoS ONE* 7: e50750

Trettel F, Rigamonti D, Hilditch-Maguire P, Wheeler VC, Sharp AH, Persichetti F, Cattaneo E, MacDonald ME (2000) Dominant phenotypes produced by the HD mutation in STHdh(Q111) striatal cells. *Hum Mol Genet* 9: 2799–2809

Trottier Y, Lutz Y, Stevanin G, Imbert G, Devys D, Cancel G, Saudou F, Weber C, David G, Tora L, Agid Y, Brice A, Mandel JL (1995) Polyglutamine expansion as a pathological epitope in Huntington's disease and four dominant cerebellar ataxias. *Nature* 378: 403–406

Wang CE, Tydlacka S, Orr AL, Yang SH, Graham RK, Hayden MR, Li S, Chan AW, Li XJ (2008) Accumulation of N-terminal mutant huntingtin in mouse and monkey models implicated as a pathogenic mechanism in Huntington's disease. *Hum Mol Genet* 17: 2738–2751

Wellington CL, Ellerby LM, Gutekunst CA, Rogers D, Warby S, Graham RK, Loubser O, van Raamsdonk J, Singaraja R, Yang YZ, Gafni J, Bredesen D, Hersch SM, Leavitt BR, Roy S, Nicholson DW, Hayden MR (2002) Caspase cleavage of mutant huntingtin precedes neurodegeneration in Huntington's disease. *J Neurosci* 22: 7862–7872

Wellington CL, Singaraja R, Ellerby L, Savill J, Roy S, Leavitt B, Cattaneo E, Hackam A, Sharp A, Thornberry N, Nicholson DW, Bredesen DE, Hayden MR (2000) Inhibiting caspase cleavage of huntingtin reduces toxicity and aggregate formation in neuronal and nonneuronal cells. *J Biol Chem* 275: 19831–19838

Wheeler VC, Auerbach W, White JK, Srinidhi J, Auerbach A, Ryan A, Duyao MP, Vrbanac V, Weaver M, Gusella JF, Joyner AL, MacDonald ME (1999) Length-dependent gametic CAG repeat instability in the Huntington's disease knock-in mouse. *Hum Mol Genet* 8: 115–122

Zala D, Hinckelmann MV, Saudou F (2013) Huntingtin's Function in Axonal Transport Is Conserved in Drosophila melanogaster. *PLoS ONE* 8: e60162

Zhang YQ, Henderson MX, Colangelo CM, Ginsberg SD, Bruce C, Wu T, Chandra SS (2012) Identification of CSPalpha clients reveals a role in dynamin 1 regulation. *Neuron* 74: 136–150